Journal of Combinatorial Mathematics
and Combinatorial Computing
www.combinatorialpress.com/jcmcc

Combinatorial Press

Study on the coupling mechanism of karst groundwater flow path to the change of hydrochemical composition in earthquake region

Min Dong[1], Qifeng Chen[1,✉], Fan Zhang[2], Jiajun Zheng[1], Bo Han[1], Fasheng Liao[1]

[1] *Shandong Seismological Bureau, Jinan, Shandong, 250000, China*
[2] *Hebei Seismological Bureau, Shijiazhuang, Hebei, 050000, China*

ABSTRACT

Water resource is a high degree of unity between quantity and quality, once the water body suffers from pollution will make the water resources more scarce, and karst groundwater resources is one of the main water resources in the seismic area. In this paper, we chose Baiquanquan area in the low-mountain hilly area at the eastern foot of the south section of Taihang Mountains in H province as the research object, set 25 sampling points and collected 20 groups of karst groundwater samples and 5 groups of surface water samples, and carried out the reliability test by the ion balance method to control the error within ±5%. Based on the karst groundwater samples, the general characteristics of its hydrochemistry were analysed, and its hydrochemical characteristics were explored by cluster analysis. The causes of hydrochemical ions in karst groundwater were investigated by Gibbs plot, chlor-alkali index and saturation index, and the related factors affecting the hydrochemical characteristics of karst groundwater were investigated by factor analysis. The hydrochemical cations and anions in karst groundwater were mainly composed of Ca^{2+} and HCO_3^-, and the average concentrations of the two were 132.15 mg/L and 193.66 mg/L, respectively.The cast points of karst groundwater all fell between the dolomite and calcite areas, and their Mg^{2+}/Ca^{2+} values ranged from 0.11 to 0.75, and the contribution of the F1 factor composed of Ca^{2+}, Mg^{2+}, SO_4^{2-}, TDS, HCO_3^- was the maximum of 38.91%. Karst groundwater in the seismic area will be affected by rock weathering, human activities, etc., which will affect the flow path of karst groundwater, and then have an impact on the hydrochemical composition of karst water.

Keywords: karst groundwater, Gibbs diagram, saturation index, factor analysis, hydrochemical composition

✉ Corresponding author.
E-mail address: smiledong2024@163.com (Q. Chen).
Received 20 February 2024; Revised 15 May 2024; Accepted 20 November 2024; Published Online 16 April 2025.
DOI: 10.61091/jcmcc127b-491

1. Introduction

Groundwater is the water present in nature in underground rocks and soil pores. The formation of groundwater is mainly related to precipitation and the groundwater cycle. When precipitation infiltrates into underground rocks and soil, part of the water evaporates or is absorbed by plants, and the remaining water enters the aquifer through infiltration and percolation, forming groundwater [1-4]. Groundwater recharge in karst areas mainly comes from precipitation infiltration and snowmelt infiltration. The storage and recharge of karst groundwater mainly occurs in groundwater storage spaces such as underground caves, fissures and karst dissolution cracks. These storage spaces usually have a large storage capacity and can rapidly draw in and release large amounts of groundwater [5-8].

Groundwater is regarded as an important geological carrier that records a variety of important information about its formation and circulation processes resulting from interactions with environmental factors, leading to different physicochemical compositional characteristics of groundwater during recharge, runoff, and discharge [9-12]. Therefore, the chemical composition of groundwater can not only reflect water quality problems and genesis mechanisms, but also play an important indicative role in identifying groundwater flow systems [13-15]. However, the multilevel nested groundwater flow systems on the regional scale make it more difficult to analyse and interpret the groundwater chemical composition data and the potential relationships among parameters due to the hierarchical and complex nature of their spatial distributions and water flow paths [16-18].

In the article, we chose Baiquanquan domain in the low-mountain hilly area in the eastern foothills of the southern section of Taihang Mountains in H province as the study area, and obtained 25 sets of karst water study samples using submersible pumps, and verified the reliability of the water sample data through the ionic equilibrium equations. Data statistics were carried out on the general characteristics of karst groundwater, including conventional physical and chemical characteristics as well as the types of hydrochemical characteristics. Cluster analysis was used to cluster the hydrochemical characteristics, and the composition of hydrochemical ions in karst groundwater was analysed by combining the Gibbs plot, the chlor-alkali index and the saturation index, and factor analysis was introduced to explore the relevant factors affecting the hydrochemical composition of karst groundwater.

2. Hydrochemical characteristics of karst groundwater in the seismic zone

Water resources are one of the indispensable natural resources for the production and life of human society, and have always played a crucial role in agriculture, industry, population growth and sustainable economic development. The demand of water resources in karst areas has become more and more prominent, and the impact of human production activities on karst groundwater systems has become more and more obvious; therefore, the rational use and development of karst water resources is an important measure for the sustainable development of human beings.

2.1. Water Sample Collection and Reliability Testing

2.1.1. Collection of karst water samples in the seismic zone. In this paper, we choose the 100 springs in the low hills of the eastern foothills of the southern section of the Taihang Mountains in Province H as the research object, whose altitude is generally in the range of 50~1100m, and the area of the springs is 3,852.7km^2, of which the indirect recharge area of the metamorphic rocks in the west is 2,184.2km^2, and the area of the distribution of the karst aquifers is 1,668.5km^2. The study area is a karst aquifer distribution area, the topography of the spring area is high in the west and low in the east, and the landform transitions from the mountainous area in the west to the hilly plain in the east, and the rivers in the area originate from the middle mountainous area in the west, and most of them are seasonal rivers, including the Baima River, the Shah River, and the Qili River.

In August 2023, 25 sets of karst groundwater samples were collected from the study area during the dry water period, including 20 sets of karst water and 5 sets of surface water. The sampling points are mainly distributed in the karst cover area where human activities are concentrated and the water-rich nature of the stratum is strong, and fewer sampling points are found in the exposed grey rock area with weak water-rich nature and large water level depth, and in the buried karst area where it is difficult to extract and use the groundwater. Groundwater samples were taken from agricultural wells and residential drinking water wells at a sampling depth of 260~700 m. The sampling equipment was a submersible pump, and if the sampling wells were being pumped and used, samples were taken directly; if they were not in normal use, more than three well volumes of groundwater were extracted prior to sampling, and the pH and conductivity parameters of the pumped water were monitored on-site, and the collection of groundwater samples started after the values had stabilised, thus eliminating the effect of standing water on the collection of samples. The samples were collected in 1000m2 of groundwater.

Each set of samples was collected in 1000mL and 250mL polyethylene bottles, of which 1000mL was used as an in-situ groundwater sample for analysis of routine chemical indicators, while 250mL samples were acidified with a superior pure HNO_3 aqueous solution to pH<3 for trace element analysis. All sample bottles were cleaned with ultrapure water before use, and then rinsed with the target water samples for 5 times before starting sampling. Groundwater samples were stored in a refrigerated box at 5°C immediately after collection and sent to the laboratory for analysis on the same day of sampling by a sample refrigerated truck.

2.1.2. Sample testing and quality control. Water temperature, conductivity, pH, redox potential and other field parameters were determined by portable multi-parameter meter (DZB-715, SH Yidian Scientific Instrument Co., Ltd.), K^+, Na^+ content was determined by atomic absorption spectrometry (A3F-15, BJ General Instrument Co., Ltd., accuracy of 0.01mg/L), Ca^{2+}, Mg^{2+} content was measured by EDTA Ca2+, Mg2+ content was determined by EDTA titration (DZ/T 0064.25), Cl^-, SO_4^{2-}, NO_3^- content was determined by ion chromatography (ICS-620, ThermoFisher, precision 0.01mg/L), HCO_3^- content, total hardness was determined by acid-base titration (DZ/T 0064, HJ 84), and the total dissolved solid (TDS) content was calculated by ion balance equation (GB/T 5750). All groundwater samples were tested by the laboratory of the Third Geological and Mineral Exploration Institute of Province H for the above indicators.

2.1.3. Reliability testing of water sample data. When using the results of water analysis, the first thing to do is to analyse the existing data and analyse the reliability of the data, on the basis of which the interpretation of some hydrogeochemical problems is more reasonable and convincing. Generally, the following methods should be taken to test the water analysis data to ensure that the data used to do a good understanding.

Macroscopically, one of the basic equilibrium conditions of aqueous solution is the condition of electroneutrality, i.e., the total number of positive ion charges in the solution is equal to the total number of negative ion charges, whose mathematical expression is:

$$\sum Z \cdot m_c = \sum Z \cdot m_a \tag{1}$$

where m_c and m_a are the molar concentrations of cations and anions, respectively, and Z is the charge of the ion, this equation is known as the electroneutrality equation. The electroneutrality equation of an aqueous solution is expressed in practical terms as the electroneutral form of its constant component:

$$\begin{aligned} &\left(\mathrm{Na}^+\right)+\left(\mathrm{K}^+\right)+2\left(\mathrm{Ca}^{2+}\right)+2\left(\mathrm{Mg}^{2+}\right) \\ &=\left(\mathrm{Cl}^-\right)+\left(\mathrm{HCO}_3^-\right)+2\left(\mathrm{CO}_3{}^{2-}\right)+2\left(\mathrm{SO}_4{}^{2-}\right) \end{aligned} \tag{2}$$

where the number is the charge of the ion and the parenthesis is the molar concentration of the ion. The formula for applying the electroneutrality equation to check the error in water analysis results is:

$$E = \left| \frac{\sum Z \cdot m_c - \sum Z \cdot m_a}{\sum Z \cdot m_c + \sum Z \cdot m_s} \right| \times 100\% \quad (3)$$

where E is the charge balance error. If $K^+ + Na^+$ is the measured value of $E < 5\%$, or $K^+ + Na^+$ is the calculated value of $E \approx 0\%$, it means that the analysis and test results are reliable, and vice versa, it means that the analysis and test results are not reliable.

There are several possible scenarios for unreliable analytical results.

1) Significant anions or cations are not included in the test data, which may indicate that some uncommon anions or cations are present in the water at higher concentrations.

2) There is a significant and systematic error in the analytical test.

3) One or more of the concentration data were recorded incorrectly.

Since the field tests and the historical data collected included multiple water sample points collected at the same or similar locations, only a representative one of these points needed to be selected as the basis for the analysis. After finishing, in the hydrochemical characterisation of karst groundwater in this study, the most representative karst water sample points in the water quality data were selected as the basis for analysis and calculation according to different analyses. After checking by the above method, the errors of the water quality analysis data of these water sample points are within the permissible range (±5%), and the analysis results are reliable and can be used in the relevant analysis and research of water chemistry in this area.

2.2. General characteristics of karst groundwater hydrochemistry

2.2.1. General physical and chemical characteristics. The chemical characteristics of water samples reflect the chemical composition of water in natural water bodies as influenced by water cycle processes and environmental interactions. Statistical analyses of water samples from the study area were carried out by counting the maximum, minimum, mean, standard deviation and coefficient of variation of the major ions. The maximum and minimum values reflect the distribution of the peaks in a set of data, the mean value is the amount of the centralised trend in a set of data, the standard deviation can show the data dispersion, and the coefficient of variation (CV) is the quotient of the standard deviation and the mean, which can show the distribution of the data and at the same time eliminate the influence of the mean value. Table 1 shows the statistical results of the testing data of karst groundwater samples in the study area.

The pH fluctuations of karst water and surface water in the study area ranged from 7.35 to 8.24 and 8.22 to 8.63, respectively, and the average pH values of karst water and surface water were 7.76 and 8.41, respectively, which were neutral alkaline water. The pH is generally low in the non-carbonate rock area due to the loss of salt-based ions from the surface under the strong rainfall drenching of the subtropical monsoon and the absorption of atmospheric or soil CO_2 by the rainwater, whereas the exogenous water in the present study area was constructed as a reservoir before sinking into the karst area, and the photosynthesis of the aquatic organisms consumed the free CO_2, which elevated the pH of the water body.

The hydrochemical cations and anions in karst groundwater were mainly composed of Ca^{2+} and HCO_3^-, with average concentrations of 132.15 and 193.66 mg/L, respectively, which together accounted for 86.15% of the total dissolved ions. The concentrations of Ca^{2+} and HCO_3^- in surface water ranged from 65.34 to 75.28 mg/L and 63.16 to 213.28 mg/L, respectively, and the concentrations of Ca^{2+} and HCO_3^- were much lower than those in karst groundwater.

The total dissolved solids (TDS) concentration of karst groundwater varied from 263.578 to 1667.42 mg/L, with a mean value of 603.48 mg/L, which was 101.79% higher than the mean value of TDS

concentration of surface water. The TDS concentrations of these two water bodies were higher than the average value of TDS concentration of more than 60 large rivers around the world (280mg/L), which is due to the fact that the study area is located in the tropical-subtropical junction area, where the rainfall is low and much lower than the evaporation, the runoff is slow, and the alternation of the water cycle is slow. According to the classification of fresh water (TDS<1g/L), brackish water (TDS in the range of 1-3g/L) and saline water (TDS>3g/L), most of the karst water in the study area belongs to fresh water and a small portion belongs to brackish water. The concentration of ions in karst groundwater water is high and the conductivity is also high. Surface water entering the karst area may have been recharged by karst groundwater or affected by human activities.

Table 1. The results of the water sample test of karst groundwater (mg/L)

Type	Index	K^+	Na^+	Ca^{2+}	Mg^{2+}	Cl-
Karst water	Max	13.12	127.65	321.57	50.15	215.43
	Min	0.26	3.67	53.48	8.42	10.92
	Means	1.47	26.98	132.15	24.97	55.37
	STD	2.39	26.35	63.04	9.51	48.06
	CV	1.65	0.99	0.46	0.35	0.91
Surface water	Max	6.45	93.42	75.28	34.37	118.67
	Min	1.31	22.68	65.34	23.25	43.59
	Means	3.98	53.45	71.26	27.86	85.48
	STD	2.14	33.08	4.67	4.69	35.79
	CV	0.56	0.62	0.07	0.16	0.43
Type	Index	SO_4^{2-}	HCO_3^-	NO_3^-	TDS	pH
Karst water	Max	155.46	406.78	233.48	1667.42	8.24
	Min	3.86	195.43	4.06	263.57	7.35
	Means	90.35	293.66	86.57	603.48	7.76
	STD	23.51	74.95	101.15	315.52	0.33
	CV	0.74	0.26	1.17	0.53	0.05
Surface water	Max	210.15	213.28	55.49	430.15	8.63
	Min	104.38	63.16	1.32	241.28	8.22
	Means	145.72	134.62	25.81	299.06	8.41
	STD	45.69	61.59	22.23	95.37	0.19
	CV	0.34	0.46	0.87	0.21	0.03

2.2.2. Types of hydrochemical characteristics. Piper's trilinear diagram has been widely used in studies to delineate the hydrochemical types of water samples and to reflect the evolution of hydrochemistry because it is not disturbed by human factors. Figure 1 shows the Piper trilinear diagram of karst groundwater and surface water in the study area.

Shukarev's classification was used to classify the hydrochemical types of karst water and surface water in the study area, and four hydrochemical types appeared in 20 sets of karst groundwater samples in the study area, of which 10 sets were of the HCO_3-Ca type, 4 sets were of the HCO_3-Ca·Mg type, and 3 sets were of the HCO_3·SO_4-Ca·Mg type, and 3 groups are HCO_3·SO_4-Ca type. It can be seen that the karst groundwater is mainly of HCO_3-Caa type, which is more obviously affected by the dissolution of carbonate rock minerals. From the recharge area at the east side of the study area to the discharge area at the outlet of the underground river at the downstream, the water chemistry type gradually changed from HCO_3-Ca type water to HCO_3·SO_4-Ca·Mg type water, and finally to HCO_3·SO_4-Ca type water at the outlet of the underground river. 5 water chemistry types appeared in 5 groups of surface water samples, and the difference between the 5 groups of surface water samples and the 5

groups of water chemistry types was very small. five water chemistry types, which are more complex compared to karst groundwater, namely HCO_3-Ca type, HCO_3-Ca·Mg type, SO_4-Ca·Mg type, HCO_3·SO_4-Ca·Mg type, SO_4-Ca type, and HCO_3-Ca type from the upstream Lanhua River - Ganxi River section to the downstream, the trend is a gradual change from HCO_3-Ca type water to HCO_3·SO_4-Ca·Mg type water. In general, the surface groundwater types in the study area reflect the characteristics of carbonate weathering.

Combined with the Piper diagrams, it can be seen that the milligram equivalent percentage of Ca^{2+} is greater than 50 per cent in all samples, with most water samples reaching more than 80 per cent of Ca^{2+}, which is distributed within the calcareous zone. Most of the cations and anions are distributed in the lower left corner and left boundary of the respective maps, which further confirms that Ca^{2+} and HCO_3^- are the dominant factors controlling the water chemistry evolution in the study area. However, the influence of seismic activities and human activities has resulted in a diversity of surface groundwater chemistry.

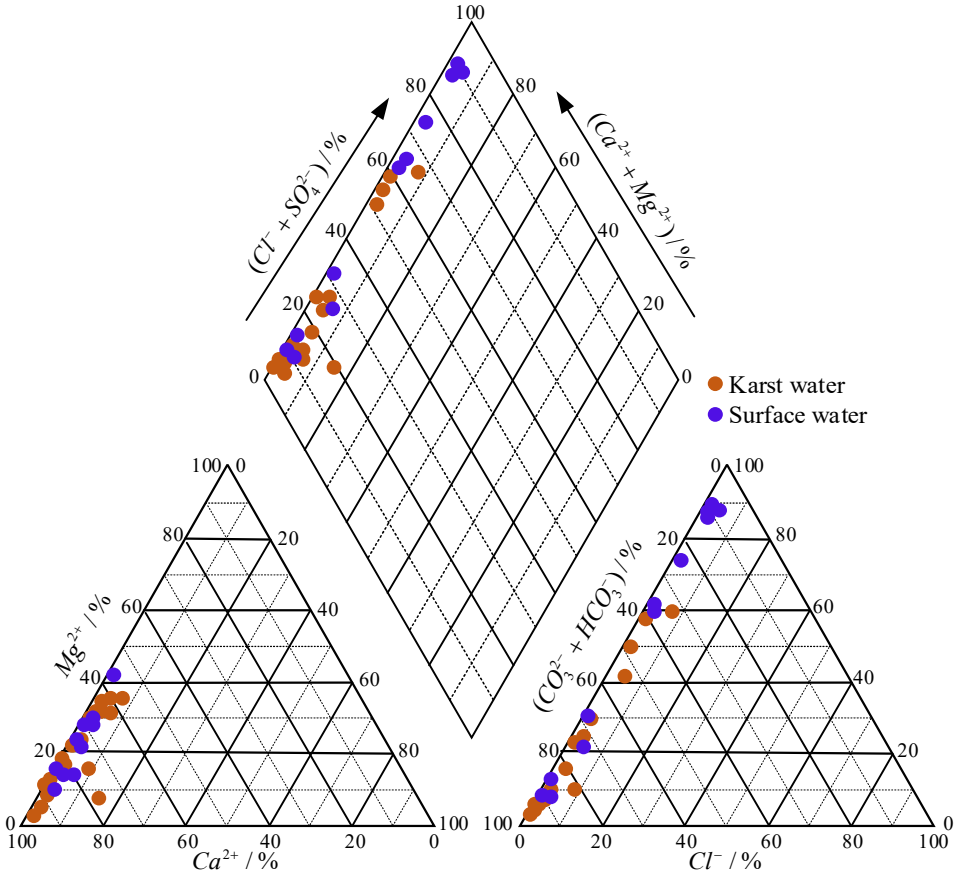

Fig. 1. Piper diagram of karst groundwater and surface water in the study area

3. Mechanisms of hydrochemical formation of karst groundwater

Water is an essential component of all life and an indispensable natural resource in the daily lives of human beings. Water resources on Earth are very rich, but freshwater resources are very scarce, accounting for only 3 per cent of the total water resources of the Earth, of which karst groundwater resources are even smaller, but their status is quite important. Karst groundwater is an important freshwater resource indispensable to the survival and development of human beings, and also an important constraint to maintain the balance of the entire natural ecosystem. The special geological structure of the seismic karst area makes its ecological vulnerability very strong, and the groundwater

environment is easily damaged. At present, people are increasingly aware of the importance of the sustainable development and use of karst groundwater resources, and how to make efficient use of karst water resources has become a fundamental solution to the production and life of residents.

3.1. Selection of research methodology

3.1.1. Cluster analysis. Cluster analysis is a new branch of multivariate statistical analysis, an analytical method that progressively groups variables (or indicators) according to their similarity to each other. According to the characteristics of the research object (samples or variables) itself, samples (variables) with high degree of similarity are grouped together by calculating the cluster statistic between them. Cluster statistics usually use distance coefficients and similarity coefficients to measure the degree of proximity between them, and there are generally three steps, i.e. standardising the data, constructing a similarity matrix between the samples, and selecting a clustering method and grouping them according to the degree of similarity [19].

According to cluster analysis the research object can be classified into R-type clustering and Q-type clustering, where R-type classifies the variables that characterise the research object, while Q-type classifies the research object itself. The results of classification are not unique, so in practical applications, different classification methods are often used to analyse and calculate the data, and combined with the background of professional knowledge, to provide specific professional analysis for the classification, and to determine the number of classifications and classification. Based on the research content of this paper, Q-type clustering is selected for the analysis of the hydrochemical formation mechanism of karst groundwater in seismic areas.

1) Data standardisation. Since the scale of the indicator variables of the research object in the actual problem often differs greatly, in order to make different data comparable, the indicator variables are usually transformed to compress the data into $[0,1]$ intervals. The formula for standard deviation transformation is as follows:

$$z_{ij} = \frac{x_{ij} - \overline{x_j}}{S_j} \tag{4}$$

where $x_j = \frac{1}{n}\sum_{i=1}^{n} x_{ij}$, $S_j = \frac{1}{n-1}\sum_{i=1}^{n}\left(x_{ij} - \overline{x_j}\right)^2$.

2) Distance calculation. To find the calculation of distance coefficient For each variable, the distance coefficient between any two of the n samples i, m is:

$$d_{im} = \sqrt{\frac{1}{n}\sum_{k=1}^{n}\left(x_{ik} - x_{mk}\right)^2}, \left(i, m = 1, 2, \cdots, n\right) \tag{5}$$

Conditional on the regularisation of the variables, $0 \le d \le 1$. obviously, the smaller the value of d, the greater the similarity between the samples. The correlation coefficients between the variables were then calculated from the standardised data and the correlation coefficient matrix was listed. The simple correlation coefficient between two variables is defined as:

$$R_{ij} = \frac{\sum_{k=1}^{n}\left(z_{ik} - \overline{z}_i\right)\left(z_{jk} - \overline{z}_j\right)}{\sqrt{\sum_{k=1}^{n}\left(z_{ik} - \overline{z}_i\right)^2 \sum_{k=1}^{n}\left(z_{jk} - \overline{z}_j\right)^2}} \tag{6}$$

Eq. $\overline{Z}_i = \frac{1}{m}\sum_{k=1}^{n} Z_{ik}$; $\overline{z}_j = \frac{1}{m}\sum_{k=1}^{n} Z_{jk}$. Finally, the spectrum of cluster analysis was plotted based on the correlation coefficient matrix on a layer-by-layer basis.

3.1.2. Factor analysis. The goal of factor analysis is to screen out a large number of samples or indicators from a small number of samples or indicators, independent of each other, and maximally representative of the main information of the subject's main factors. Factor analysis is usually divided into Q-type factor analysis and R-type factor analysis, Q-type factor analysis is generally used for the study of samples, while R-type factor analysis is generally used for the study of sample indicators [20]. In this paper, the steps of using R-type factor analysis are as follows:

1) Data pre-processing. In order to eliminate quantitative differences, the aim was to obtain a standardised matrix of water chemistry data matrices. It is assumed that the study population contains n sample with m variables per sample, composing the matrix X as:

$$X = \begin{bmatrix} x_{11} & x_{12} & \cdots & x_{1m} \\ x_{21} & x_{22} & \cdots & x_{2m} \\ \vdots & \vdots & \vdots & \vdots \\ x_{n1} & x_{n2} & \cdots & x_{nm} \end{bmatrix} \tag{7}$$

Represent the above variables as a linear relationship where each variable contains the common factor $F\left(F_1, F_2, \ldots, F_p; p < m\right)$ and the respective special factor $\varepsilon\left(\varepsilon_1, \varepsilon_2, \cdots, \varepsilon_p\right)$. i.e.:

$$\begin{cases} x_1 = a_{11}F_1 + a_{12}F_2 + \cdots + a_{1p}F_p + a_1\varepsilon_1 \\ x_2 = a_{21}F_1 + a_{22}F_2 + \cdots + a_{2p}F_p + a_2\varepsilon_2 \\ \vdots \\ x_m = a_{m1}F_1 + a_{m2}F_2 + \cdots + a_{mp}F_p + a_m m \end{cases} \tag{8}$$

where x_i is the i nd initial variable, a_{ij} is the factor loadings, ε is the special factor, and F is the common factor.

2) Normalisation of the factor loading matrix:

$$x_{ij}' = \frac{x_{ij} - \overline{x}_j}{S_j}\left(i = 1, 2.3, \ldots, n; j = 1, 2, 3, \ldots, m\right) \tag{9}$$

where $\overline{x}_j$ is:

$$\overline{x}_{ij} = \frac{1}{n}\sum_{i=1}^{n} x_{ij}; S_j = \sqrt{\left(\frac{1}{n}\sum_{i=1}^{n}\left(x_{ij} - \overline{x}_i\right)^2\right)} \tag{10}$$

where S_j is:

$$S_j = \frac{1}{n}\sum_{k=1}^{n}\left(x_{ki} - \overline{x}_i\right)\left(x_{ij} - \overline{x}_j\right)\left(i = 1, 2.3, \ldots, n; j = 1, 2, 3, \ldots, m\right) \tag{11}$$

3) Calculate the correlation matrix R of the standard matrix, where the correlation coefficient r_{jk} is:

$$r_{jk} = \frac{\sum_{i=1}^{n} x_{ij} x_{ik}}{n} \left(i = 1, 2.3, \ldots, n; j = 1, 2, 3, \ldots, m\right) \tag{12}$$

4) Compute the eigenvectors and eigenvalues of matrix R. Assuming that B is a square matrix of order n and X is a n-dimensional non-zero column vector, the eigenvalue λ of square matrix B can be calculated as follows:

$$\left(B - \lambda I_n\right) X = 0 \tag{13}$$

where I_n is a unit matrix of order n and the number of eigenvalues is equal to the number of variables.

Eigenvector X is calculated as:

$$RX - \lambda X = 0 \tag{14}$$

5) Calculate the contribution q and cumulative contribution Q of eigenvalues to select eigenvalues. i.e:

$$q = \frac{\lambda_i}{\sum_{i=1}^{m} \lambda_i} \left(i = 1, 2.3, \ldots, m\right) \tag{15}$$

$$Q = \sum_{j=1}^{k} \frac{\lambda_i}{\sum_{i=1}^{m} \lambda_i} \left(k \le m\right) \tag{16}$$

6) Calculate the factor loadings and derive the loading matrix A as:

$$a_{ij} = X_{ij} \sqrt{\lambda_i} \left(i = 1, 2.3, \ldots, n; k = 1, 2, 3, \ldots, m\right) \tag{17}$$

where X_{ij} is the j rd eigenvector corresponding to the i nd eigenvalue and k is the number of eigenvalues.

The initial factor loading matrix A is:

$$A = \begin{bmatrix} a_{11} & a_{12} & \ldots & a_{1m} \\ a_{21} & a_{22} & \ldots & a_{2m} \\ \vdots & \vdots & \vdots & \vdots \\ a_{n1} & a_{n2} & \ldots & a_{nm} \end{bmatrix} \tag{18}$$

7) Factor rotation. Factor rotation can be performed when the initial factor loading matrix is not easy to interpret the main factors to carry out, factor rotation can make the structure of the factor loading matrix simplified and easy to interpret.

3.1.3. Gibbs diagram. Gibbs plots were used to qualitatively analyse the mechanisms of origin of various ions in groundwater. The distribution of the ratio of the vertical coordinate TDS content to the horizontal coordinate $Cl^- / (Cl^- + HCO_3^-)$ or $Na^+/(Na^+ + Ca^{2+})$ content classifies the controlling factors for the chemical components of natural water as evaporation and concentration, rock weathering, or the action of atmospheric precipitation. When the dominant process is atmospheric precipitation, TDS values are low and $Cl^- / (Cl^- + HCO_3^-)$ or $Na^+/(Na^+ + Ca^{2+})$ is high, and the sample data are in the lower right corner of the graph [21].

In order to understand the ion exchange between the groundwater and the aquifer, the chloralkali

index CAI-1 was calculated for the groundwater samples, which is usually calculated using the following formula:

$$CAI-1=\frac{\gamma Cl^{-}-\left(\gamma Na^{+}+\gamma K^{+}\right)}{\gamma Cl^{-}} \tag{19}$$

where γ is the ion equivalent concentration $\left(meq/L\right)$. The chlor-alkali indicator CAI-1 is commonly used to characterise the direction and strength of cation exchange interactions [22].

3.1.4. Saturation factor. The saturation index (SI) is a hydrogeochemical indicator used to describe the saturation state of minerals in groundwater. When SI=0, the minerals are in dissolution-precipitation equilibrium, if SI<0 the minerals are not saturated, i.e., they are in a dissolved state, and if SI>0 it indicates that the minerals are in a supersaturated state, i.e., the minerals will precipitate and precipitate out [23].

The saturation index of minerals in water is defined as:

$$SI=\lg\frac{IAP}{K} \tag{20}$$

where IAP is the activity product, the value of which is the product of the ionic activity coefficient γ_i and the concentration of the component m_i, and K is the equilibrium constant of the mineral at a given temperature.

For the following reaction equation:

$$aA \Leftrightarrow dD+eE \tag{21}$$

It can be written according to the reaction free energy equation:

$$-\Delta G_r=RT\ln\frac{\left[D\right]^d\left[E\right]^e}{\left[A\right]^a}-RT\ln K_a \tag{22}$$

If the A term in Eq. is a solid, then Eq. can be written as:

$$\Delta G_r=-RT\ln\frac{\left[D\right]^d\left[E\right]^e}{K_{rp}} \tag{23}$$

$$LAP=\left[D\right]^d\left[E\right]^e \tag{24}$$

$$\Delta G_r=-2.303RT\lg\frac{IAP}{K_{yp}} \tag{25}$$

$$SI=\frac{-\Delta G_r}{2.303RT} \tag{26}$$

From the above equation, SI is a function of ΔG_z. If $\Delta G_z=0$, then $SI=0$, the reaction is at equilibrium, if $\Delta G_x<0$, then $SI>0$, the reaction proceeds spontaneously to the right and the mineral is in the dissolved state, and if $\Delta G_x>0$, then $SI<0$, the reaction proceeds spontaneously to the left and the mineral is in the precipitated state.

3.2. Hydrochemical causes of karst groundwater

3.2.1. Cluster analysis of water chemistry characteristics. Cluster analysis can cluster the similarity of the analysed variables or dataset attributes, and the results of the analysis are presented in the form of cluster dendrograms, which have been widely used to reveal the correlation between hydrochemical

factors, i.e., hydrochemical ions clustered together into one class, which indicates that these ions have a similar hydrogeochemical evolutionary process. Based on the method of Q-type cluster analysis given in the previous section, when taking the eigenvalue of the cluster dendrogram as 12, the results of hierarchical cluster analysis of the hydrochemical characteristics of karst groundwater in the study area are obtained as shown in Fig. 2.

The chemical ions in karst groundwater in the study area can be divided into four different clusters. Cluster 1 clusters TDS, Ca^{2+} and HCO_3^- in karst groundwater in the study area into one group, Ca^{2+} and HCO_3^- are usually affected by anthropogenic discharges to a low degree, and are mainly controlled by the strong dissolution of calcite. And Ca^{2+} and HCO_3^- are the dominant ions, affecting the TDS level of karst groundwater, so cluster 1 can characterise the strong water-rock action. Cluster 2 clusters Mg^{2+}, F^- and SO_4^{2-} in the karst groundwater of the study area into one class, and these ions in karst groundwater usually come from the weak hydrological rock dissolution of minerals such as dolomite [$CaMg(CO_3)_2$], fluorspar (CaF_2), and gypsum ($CaSO_4$), etc., and the concentrations of these ions in the other sampling sites are low, so Cluster 2 can characterise the weak hydrological rock action. Cluster 3 clusters K^+, Cl^-, Na^+ and NO_3^- in the karst groundwater in the study area into one group, of which K^+ and NO_3^- have typical characteristics of agricultural activities, and Cl- and Na+ usually have characteristics of domestic wastewater and industrial production discharge, so Cluster 3 mainly reflects the impact of anthropogenic discharge on the chemistry of karst groundwater. Cluster 4 clusters NO_2^- and NH_4^+ in karst groundwater in the study area into one group, and the detection rates of these two ions are 58.47% and 22.06%, respectively, and their average concentrations are much lower than those of other ions, so Cluster 3 is characterised as a low-concentration component. Based on different clusters, we can better analyse the reasons for the formation of different types of hydrochemical features, and provide support for exploring the formation mechanism of hydrochemical ions.

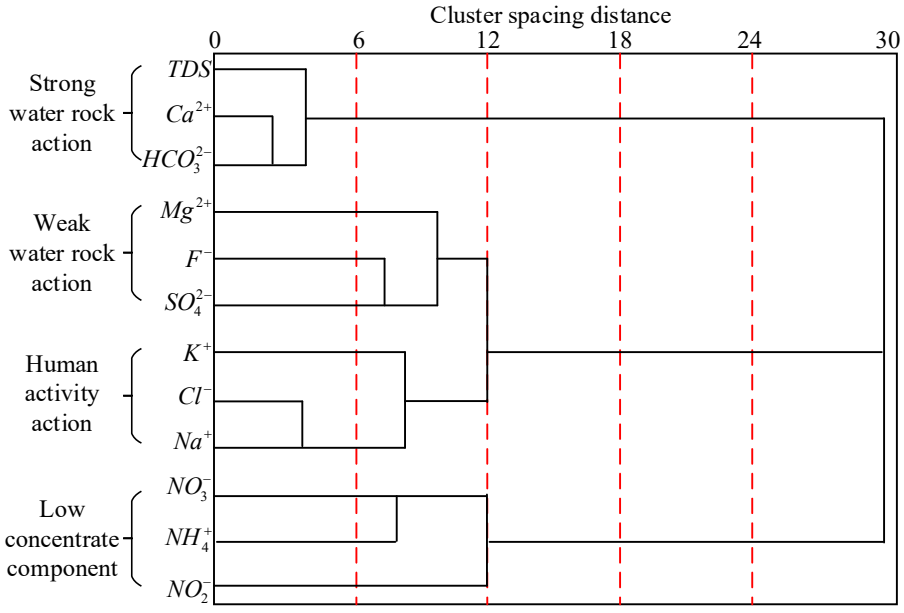

Fig. 2. Clustering analysis of hydration characteristics

3.2.2. Hydrochemical causes of karst groundwater:

1) Role of water and rock. The pH value of karst groundwater in the study area ranges from 7.35 to 8.24, which is neutral alkaline water, and the hydrochemical characteristics of karst groundwater in the rock study area generally show similar characteristics. It has been shown that the soluble ionic components of karst groundwater mainly come from three aspects: chemical weathering of rocks,

atmospheric input (rainfall), and evaporation and concentration effects. The Gibbs diagram of groundwater can be used to qualitatively describe the origins and change trends of groundwater components. The relevant ion content of the karst groundwater in the study area was put into the Gibbs diagram, and Fig. 3 shows the Gibbs diagram of the karst groundwater in the study area. Among them, Fig. 3(a)~(b) are the $Na^+/(Na^+ + Ca^{2+})$ Gibbs plots of $Cl^- / (Cl^- + HCO_3^-)$, respectively. It can be seen that the karst groundwater in the study area is concentrated in the rock-weathering type area, indicating that the karst groundwater in the study area is mainly 'rock-weathering type' groundwater, and its ionic components are mainly derived from the weathering and dissolution of soluble carbonate rocks.

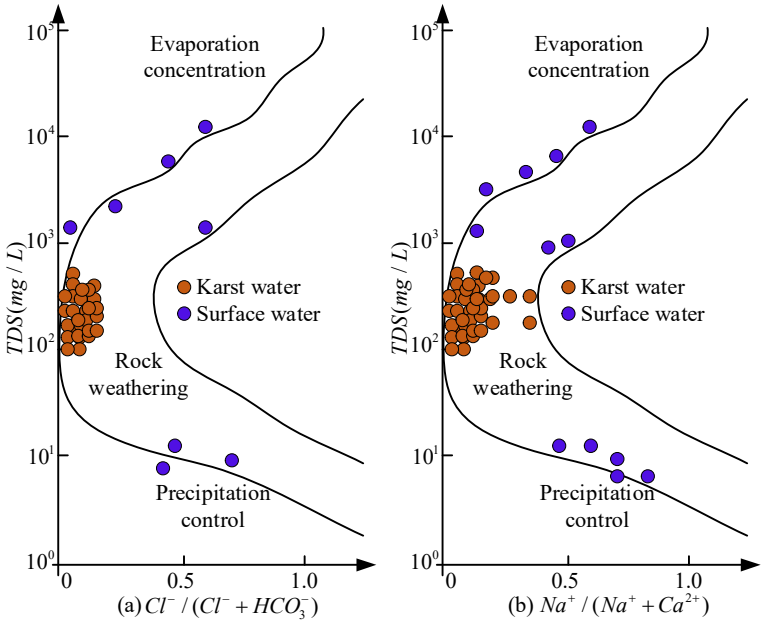

Fig. 3. The karst groundwater Gibbs diagram

Ca^{2+}, HCO_3^- and Mg^{2+} ions in karst groundwater in the study area mainly originate from the dissolution and erosion of carbonate rocks, while the Mg^{2+}/Ca^{2+} values are mainly controlled by the proportion of calcite and dolomite contained in soluble carbonate rocks. The relationship of $HCO_3^- - (Mg^{2+} / Ca^{2+})$ in karst groundwater is shown in Fig. 4. From the figure, it can be seen that the cast points of karst groundwater in the study area all fall between the dolomite and calcite areas, and their Mg^{2+}/Ca^{2+} values range from 0.11 to 0.75, with very few water samples having Mg^{2+}/Ca^{2+} ratios greater than 0.75. This indicates that the Ca^{2+}, HCO_3^- and Mg^{2+} in karst groundwater in the study area are all supplied by the dissolution filtration of dolomite and calcite minerals.

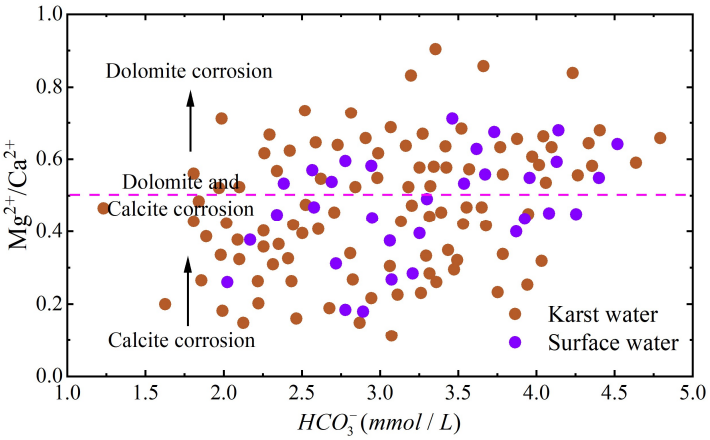

Fig. 4. Relationship of $HCO_3^- - (Mg^{2+}/Ca^{2+})$

The process of water-rock action of karst groundwater is dominated by carbonic acid dissolution of carbonate rock, when carbonate rock is only dissolved by carbonic acid, the theoretical molar ratio of $(Mg^{2+}/Ca^{2+})/HCO_3^-$ in groundwater is 0.45, and nitric acid and sulfuric acid brought in by human production and life can also dissolve carbonate rock to different degrees, resulting in changes in the $[SO_4^{2-}/HCO_3^-]$ - $(Mg^{2+}/Ca^{2+})/HCO_3^-$ molar ratio in groundwater. Figure 5 shows the relationship between $[SO_4^{2-}/HCO_3^-]$ - $(Mg^{2+}/Ca^{2+})/HCO_3^-$ of karst groundwater in the study area. As can be seen from the figure, the molar ratios of $[SO_4^{2-}/HCO_3^-]$ - $(Mg^{2+}/Ca^{2+})/HCO_3^-$ and $(Mg^{2+}/Ca^{2+})/HCO_3^-$ are mostly lower than 0.9, and the casting points are all concentrated in the lower left corner of the figure, and there is a tendency for individual samples to evolve towards the gypsum dissolution line. In particular, two groups of water samples, the descending spring on the water head in Hongma Village, Township Y, and the descending spring on Longyan Slope in Yankou Village, Township J, fall on the right side of the gypsum dissolution line and its vicinity, which shows that they are significantly controlled by gypsum dissolution.

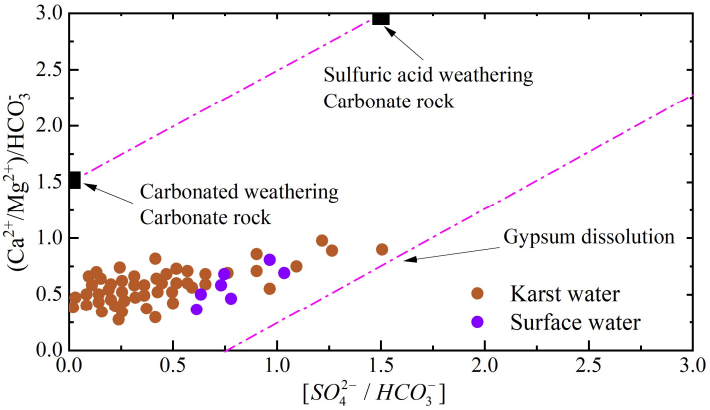

Fig. 5. Relationship of $[SO_4^{2-}/HCO_3^-]-(Mg^{2+}/Ca^{2+})/HCO_3^-$

2) Cation exchange and anthropogenic effects. The milligram equivalence ratio of Na^+ and Cl^- can reflect the water-rock interaction during karst groundwater runoff. Normally, if all Na^+ and Cl^- in groundwater are derived from dissolved Na^+/Cl^- of rock salt, the equivalence ratio should be 1. Fig. 6 shows the relationship between Na^+/Cl^- in karst groundwater in different areas of the study area (East Zone and West Zone). It can be seen from the figure that the Na^+ and Cl^- contents in the groundwater in the East Zone are significantly higher than those in the West Zone, and some water samples are located above the 1:1 isobar, and the excess Na^+ may be related to silicate dissolution or cation

exchange action, whereas the silicate content in the carbonate rock strata is low. Therefore, it may be influenced by cation exchange action, which leads to the increase of Na^+ content in groundwater.

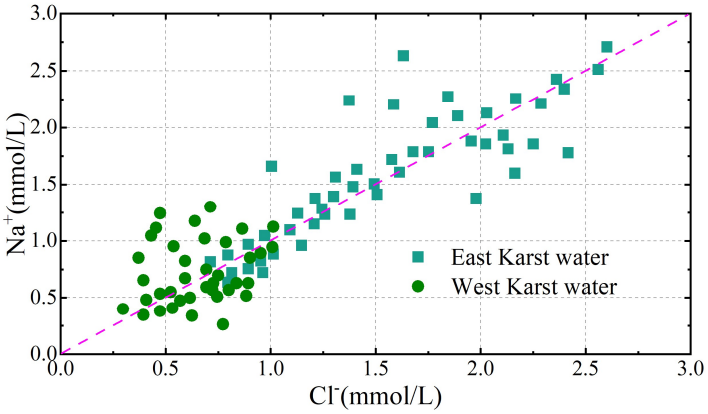

Fig. 6. Plots of Na^+/Cl^- in the study area

In order to further explore the cation exchange, based on the calculation method of chlor-alkali index given in the previous section, it is used to judge the positive and negative reactions of Ca^{2+}, Mg^{2+} and K^+, Na^+ mutual substitution in karst groundwater. When CAI-1 is positive, it means that the ion exchange reaction between K^+ and Na^+ in karst groundwater and Ca^{2+} and Mg^{2+} in the aquifer is reverse ion exchange, and when CAI-1 is negative, it means that the ion exchange reaction between Ca^{2+} and Mg^{2+} in the groundwater and K^+ and Na^+ in the aquifer is positive ion exchange. Figure 7 shows the calculation results of chlor-alkali index of karst groundwater in the study area. As can be seen from Fig. 7, the chlor-alkali index of some groundwaters in the study area is distributed in both positive and negative regions. It indicates that both positive and reverse ion exchange reactions occur in the aquifer, and the intensity of positive ion exchange is larger, which is mainly related to the higher content of Ca^{2+} and Mg^{2+} in the carbonate aquifer.

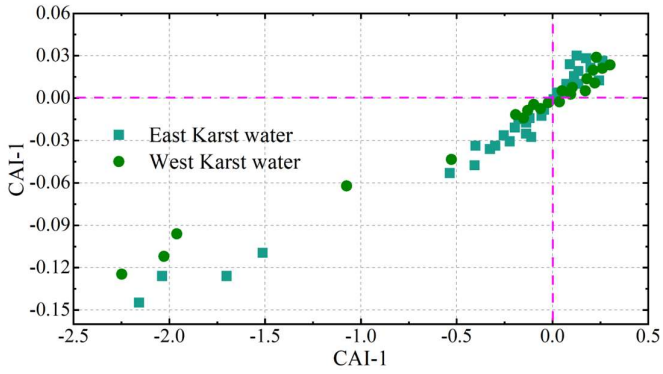

Fig. 7. Calculation results of groundwater chlorinated index

With regard to the sources of water chemical ions in karst groundwater, in addition to water-rock interaction and cation exchange, the pollution of the groundwater environment by human activities, especially industrial and agricultural production, has become increasingly serious. A large number of studies have found that NO_3^-, Cl^- and SO_4^{2-} can reflect the impact of anthropogenic inputs on the groundwater environment. In this regard, this paper analyses the relevance of human activities on the generation of hydrochemical ions in karst groundwater. Figure 8 shows the correlation between NO_3^- / Na^+ and Cl^- / Na^+ in karst groundwater.

According to the results of correlation analysis, the correlation coefficients of Cl^- and NO_3^- in karst groundwater in the west and east zones are 0.841 and 0.816, respectively, with obvious correlation,

and generally water sample sites with high Cl- content are also significantly high in NO_3^- content. Heavily anthropogenically contaminated groundwater is usually accompanied by high NO_3^- / Na^+ and Cl^- / Na^+. Rock weathering contributes little to groundwater NO_3^- and Cl^-, and lower NO_3^- / Na^+ and Cl^- / Na^+ are defined as the weathering end elements of carbonates and silicates. Karst groundwater samples are mainly distributed near the end elements of agricultural activities, indicating that the groundwater in the study area is highly influenced by human activities. The study area is in an area of intensive human activities, and domestic sewage and agricultural fertilisers are the main contributors to the elevated NO_3^- content of groundwater in the east.

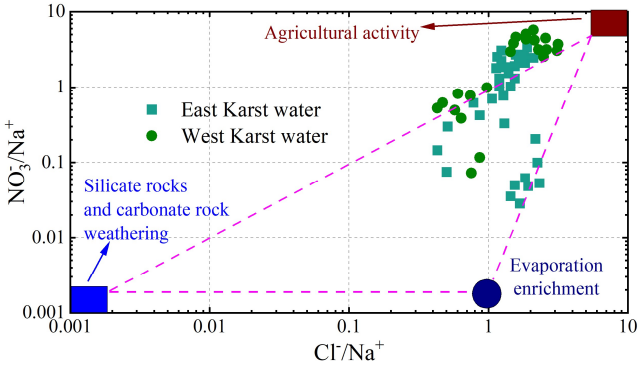

Fig. 8. Relationship of between NO_3^- / Na^+ and Cl^- / Na^+

3) Saturation coefficient of karst groundwater. Calculating the saturation indices of minerals such as rock salt (NaCl), gypsum ($CaSO_4 \cdot 2H_2O$), calcite ($CaCO_3$), and dolomite ($CaMg(CO_3)_2$) in the karst aquifer can further determine whether dissolution and filtration are occurring in the karst groundwater in the study area. Due to certain errors in the water quality analysis, mineral equilibrium constants and ionic activity calculations, which lead to certain uncertainties in the results of the SI calculations, the minerals can be considered to be in equilibrium relative to the aqueous solution when the variation of the SI is in the range of ±0.5. Using PHREEQC software to calculate the SI of different minerals in karst groundwater in the study area, the relationship between SI and TDS of major minerals in karst groundwater in the study area was obtained as shown in Figure 9.

From the figure, it can be seen that the SI of saltpeter (NaCl) in the karst aquifer in the study area varies from -5.71 to -3.74, the SI of calcite ($CaCO_3$) varies from -0.93 to 0.97, the SI of dolomite ($CaMg(CO_3)_2$) varies from -0.99 to 1.18, and the SI of gypsum ($CaSO_4 \cdot 2H_2O$) had SI variations ranging from -4.81 to -0.72. The SI of both rock salt and gypsum in the groundwater was less than 0, indicating that they were in a dissolved state. The SI of calcite and dolomite in both near 0, showing a dissolved/precipitated state. In addition, with the increase of TDS, the SI of each mineral showed an increasing trend. In conclusion, it is further confirmed that calcite and dolomite in carbonate minerals, and gypsum and rock salt in evaporite minerals are the main ionic sources of karst groundwater in the study area.

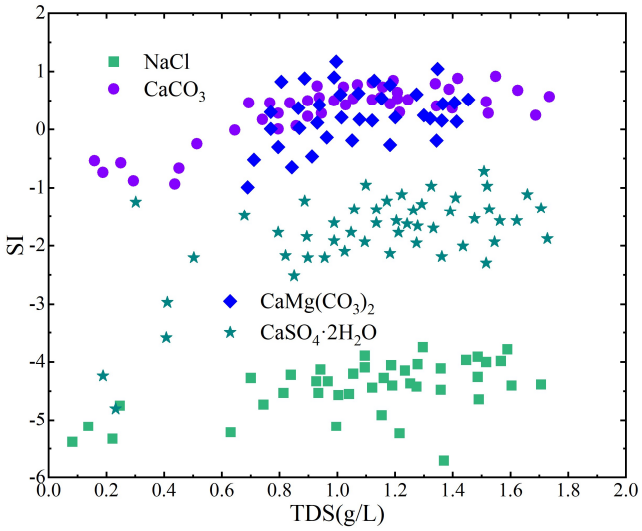

Fig. 9. The relationship between major mineral SI and TDS

3.2.3. Factors affecting water chemistry characteristics. In order to further determine the controlling factors of the hydrochemical components of karst water, factor analysis was carried out using SPSS software. A total of 9 indicators, Ca^{2+}, Mg^{2+}, Cl^-, SO_4^{2-}, HCO_3^-, TDS, NO_3^-, Na^+ and K^+, were selected for analysis. The measured values of each indicator were standardised and then subjected to the KMO-Bartlett spherical test, and the significance level was close to 0, indicating that there was a strong correlation between the indicator variables, which met the test criteria and allowed for principal component analysis. The results of the analyses were used to further grasp the influence of factors such as natural conditions and anthropogenic activities on the hydrochemical composition of karst water in the study area. The principal component analysis and factor analysis were sorted out, and the principal component variance explainable quantity of the main ions of karst groundwater in the study area as well as the rotated component matrix were shown in Tables 2 and 3, respectively. Var and CVC in the table represent the variance contribution rate and cumulative variance contribution rate, respectively, and the unit is %.

The factor contribution of F1 was 38.91%, and the main loadings were Ca^{2+}, Mg^{2+}, SO_4^{2-}, TDS, HCO_3^- and all of them were positively correlated with F1, and their factor loadings exceeded 0.8. This indicated that HCO_3^- the concentration significantly affected the hydrogeochemical processes of the water body, and carbonate was widely involved in the hydrogeochemical processes of the local karst water. HCO_3^- The two main sources are the oxidative dissolution of Carboniferous-Permian pyrite (pit water) and recharge to karst water, and the discharge of mine wastewater to surface water after evacuation to the mine wastewater treatment station to meet the standard and recharge to groundwater during runoff along the route. Thus, the F1 factor represents the influence of pit water on the chemical components of water.

The contribution of F2 factor was 18.85% and the main loadings were Na^+, K^+ and Cl^-. Strong alternating cation adsorption exists in the study area and is widely involved in the hydrogeochemical processes of karst water. Among them, the higher concentrations of Na^+ and K^+ are due to the cation back-exchange effect when the karst water of Ordovician chert containing Ca^{2+} and Mg^{2+} ions flows through the rock and soil with adsorbed Na^+ and K^+, which makes the concentration of Na^+ in the groundwater increase and the concentration of Ca^{2+} and Mg^{2+} ions decrease. At the same time, due to the dissolution of salt rock, the concentration of Cl^- is increasing, and the concentration of Cl^- and Na^+ is increasing at the same time, the karst water shows the characteristic of 'salinisation'. The F2 factor represents the effect of cationic back-exchange on the chemical components of water.

The contribution rate of F3 factor is 16.72%, and the main loadings are K^+ and NO_3^-. Sampling points with high contribution rate of F3 factor are mostly located in towns where human activities are

concentrated, so F3 factor is related to the application of fertiliser in agricultural activities and direct discharge of sewage from residents' domestic life.

Table 2. The main component variance of the main ions can be explained

Factor	Initial eigenvalue			Extraction eigenvalue			Rotational eigenvalue		
	Total	Var	CVC	Total	Var	CVC	Total	Var	CVC
1	4.516	40.44	40.44	4.516	40.44	40.44	4.345	38.91	38.91
2	2.043	18.29	58.73	2.043	18.29	58.73	2.105	18.85	57.76
3	1.759	15.75	74.48	1.759	15.75	74.48	1.867	16.72	74.48
4	1.205	10.79	85.27	-	-	-	-	-	-
5	0.872	7.81	93.08	-	-	-	-	-	-
6	0.638	5.71	98.79	-	-	-	-	-	-
7	0.105	0.94	99.73	-	-	-	-	-	-
8	0.027	0.24	99.97	-	-	-	-	-	-
9	0.003	0.03	100.00	-	-	-	-	-	-

Table 3. The component matrix after rotation

Variable	Factor		
	1	2	3
Ca^{2+}	**0.881**	-0.335	-0.262
Mg^{2+}	**0.842**	-0.214	-0.289
Cl^{-}	-0.435	**0.783**	-0.351
SO_4^{2-}	**0.906**	-0.224	-0.114
HCO_3^-	**0.958**	-0.036	-0.028
TDS	**0.973**	-0.081	-0.056
NO_3^-	-0.249	-0.458	**0.732**
Na^{+}	-0.573	**0.747**	-0.347
K^{+}	-0.108	**0.732**	**0.718**

4. Conclusion

With regard to the changes in the hydrochemical composition of karst groundwater in the seismic area, the paper draws the following conclusions:

1) The hydrochemical cations and anions in karst groundwater are mainly composed of Ca^{2+} and HCO_3^-, with average concentrations of 132.15 and 193.66 mg/L respectively, accounting for 86.15% of the total dissolved ions. The concentration ranges of Ca^{2+} and HCO_3^- in surface water were 65.34-75.28 mg/L and 63.16-213.28 mg/L, respectively, and the concentrations of Ca^{2+} and HCO_3^- were much lower than those in karst groundwater. The milligram equivalent percentage of Ca^{2+} was greater than 50% in all samples, and most of the water samples had a milligram equivalent percentage of Ca^{2+} of more than 80%, distributed within the calcareous zone.

2) All the casts of karst groundwater in the study area fall between the dolomite and calcite areas, and their Mg^{2+}/Ca^{2+} values range from 0.11 to 0.75, with very few water samples having Mg^{2+}/Ca^{2+} ratios greater than 0.75, suggesting that the Ca^{2+}, HCO_3^- and Mg^{2+} of the karst groundwater in the study area are provided by the dissolution and filtration of dolomite and calcite minerals.

3) The SI of calcite ($CaCO_3$) and dolomite ($CaMg(CO_3)_2$) varied between -0.93 and 0.97 and -0.99 and 1.18, respectively, and both of them were in dissolved/precipitated state. Calcite and dolomite in carbonatite minerals, and gypsum and rock salt in evaporite minerals are the main ionic sources of karst groundwater in the study area.

4) The factors affecting the hydrochemical composition of karst groundwater in the seismic area

mainly include Ca^{2+}, Mg^{2+}, Cl^-, SO_4^{2-}, HCO_3^-, TDS, NO_3^-, Na^+, K^+, and nine indicators, among which the F1 factor composed of Ca^{2+}, Mg^{2+}, SO_4^{2-}, TDS, and HCO_3^- contributes the most to 38.91%.

Clarifying the characteristics of the hydrochemical composition of karst groundwater in the seismic area and the influencing factors can help to better develop karst groundwater and improve the utilisation rate of karst groundwater resources.

References

[1] Vo-Van, T., Nguyen-Hai, A., Tat-Hong, M. V., & Nguyen-Trang, T. (2020). A new clustering algorithm and its application in assessing the quality of underground water. Scientific Programming, 2020(1), 6458576.

[2] Liang, J., Huang, X., Yan, J., Li, Y., Zhao, Z., Liu, Y., ... & Wei, Y. (2021). A review of the formation of Cr (VI) via Cr (III) oxidation in soils and groundwater. Science of The Total Environment, 774, 145762.

[3] Jing, X. Y., Yang, H., Cao, Y., & Wang, W. (2014). Identification of indicators of groundwater quality formation process using a zoning model. Journal of Hydrology, 514, 30-40.

[4] Grinevskii, S. O. (2014). The effect of topography on the formation of groundwater recharge. Moscow University Geology Bulletin, 69, 47-52.

[5] Bakalowicz, M. (2015). Karst and karst groundwater resources in the Mediterranean. Environmental Earth Sciences, 74, 5-14.

[6] Kalhor, K., Ghasemizadeh, R., Rajic, L., & Alshawabkeh, A. (2019). Assessment of groundwater quality and remediation in karst aquifers: A review. Groundwater for sustainable development, 8, 104-121.

[7] Bonacci, O. (2015). Surface waters and groundwater in karst. Karst aquifers—characterization and engineering, 149-169.

[8] Gunn, J. (2021). Karst groundwater in UNESCO protected areas: a global overview. Hydrogeology Journal, 29(1), 297-314.

[9] Lerner, D. N. (2020). Groundwater recharge. In Geochemical processes, weathering and groundwater recharge in catchments (pp. 109-150). CRC Press.

[10] Dzhamalov, R. G., Frolova, N. L., Kireeva, M. B., & Safronova, T. I. (2010). Climate-induced changes in groundwater runoff in Don Basin. Water Resources, 37, 733-742.

[11] Luijendijk, E., Gleeson, T., & Moosdorf, N. (2020). Fresh groundwater discharge insignificant for the world's oceans but important for coastal ecosystems. Nature communications, 11(1), 1260.

[12] Otieno, F. A. O., Olumuyiwa, I. O., & Ochieng, G. M. (2012). Groundwater: Characteristics, qualities, pollutions and treatments: An overview. African journal of agricultural research.

[13] Subba Rao, N., Marghade, D., Dinakar, A., Chandana, I., Sunitha, B., Ravindra, B., & Balaji, T. (2017). Geochemical characteristics and controlling factors of chemical composition of groundwater in a part of Guntur district, Andhra Pradesh, India. Environmental earth sciences, 76, 1-22.

[14] Dragon, K., & Marciniak, M. (2010). Chemical composition of groundwater and surface water in the Arctic environment (Petuniabukta region, central Spitsbergen). Journal of Hydrology, 386(1-4), 160-172.

[15] Tarasenko, I., Kholodov, A., Zin'kov, A., & Chekryzhov, I. (2022). Chemical composition of groundwater in abandoned coal mines: Evidence of hydrogeochemical evolution. Applied Geochemistry, 137, 105210.

[16] Tikhomirov, V. V. (2016). Hydrogeochemistry Fundamentals and Advances, Groundwater Composition and Chemistry (Vol. 1). John Wiley & Sons.

[17] Liu, J., Hao, Y., Gao, Z., Wang, M., Liu, M., Wang, Z., & Wang, S. (2019). Determining the factors controlling the chemical composition of groundwater using multivariate statistics and geochemical methods in the Xiqu coal mine, North China. Environmental Earth Sciences, 78, 1-11.

[18] Eyankware, M. O. (2019). Hydrogeochemical assessment of chemical composition of groundwater; A case study of the aptian-albian aquifer within sedimentary basin (Nigeria). Water Conservation and Management, 3(1), 01-07.

[19] Evangelos Tziritis,Ekaterini Sachsamanoglou & Cüneyt Güler. (2024). Evaluating spatiotemporal groundwater quality changes in the Rhodope coastal aquifer system (NE Greece) employing a GIS-assisted hybrid approach of multivariate statistics and inverse geochemical modeling. The Science of the total environment174676.

[20] Machado Carlos José Freire,Santiago Maria Marlúcia Freitas,Frischkorn Horst & Filho Josué Mendes. (2018). Clustering of groundwaters by Q-mode factor analysis according to their hydrogeochemical origin: A case study of the Cariri Valley (Northern Brazil) wells. Water SA(5),651-651.

[21] Biswas Tanmoy,Pal Subodh Chandra,Ruidas Dipankar,Saha Asish,Shit Manisa,Islam Abu Reza Md. Towfiqul... & Costache Romulus. (2023). Evaluation of groundwater contamination and associated human health risk in a water-scarce hard rock-dominated region of India: Issues, management measures and policy recommendation. Groundwater for Sustainable Development.

[22] Shipra Tyagi & Kiranmay Sarma. (2020). Qualitative assessment, geochemical characterization and corrosion-scaling potential of groundwater resources in Ghaziabad district of Uttar Pradesh, India. Groundwater for Sustainable Development(prepublish),100370-100370.

[23] Emmanuel Aguiza Abaï,Hugues Pahimi,Prosper Samba Koukouare,Guillaume Ewodo Mboudou & Auguste Ombolo. (2024). Hydrochemistry of Groundwater in the Rice Cultivation Area of Maga: Analysis of the Mineralization Process. Journal of Geoscience and Environment Protection(09),370-387.